IMPROVEMENTS IN ULTRASONIC MEASUREMENT MODELING WITH APPLICATIONS TO ULTRASONIC RELIABILITY

T. A. Gray, R. B. Thompson and B. P. Newberry

Ames Laboratory, USDOE
Iowa State University
Ames, IA 50011

INTRODUCTION

Over the past several years, work has been reported on the development and implementation of a measurement model relating measured ultrasonic signals obtained through planar or cylindrically curved interfaces to far field scattering amplitudes (1). A number of applications have also been described, including obtaining scattering amplitudes (2) to improve sizing capability via the inverse Born approximation (3), predicting detected signals from cracks in planar (4) and cylindrical (5) geometries, and establishing detection filters (6) for improved inspectability. These applications have used models of diffraction effects for the case of piston source radiation (7) which were developed to account only for the axial pressure fields. A number of desired applications such as treating large flaws and scanning modes will require the ability to model the full radiation field of a probe. As a first step, a model of the radiation of Gaussian profile probes through planar or curved surfaces has been developed (8). With suitable normalization, this model can be used to predict the far-field behavior of piston probes. This allows modeling of full field behavior near the focal region of either focussed probes or focussing part surfaces. This paper will discuss the incorporation of the Gaussian beam theory into the measurement model. Also reported will be several new applications of the measurement model to problems associated with ultrasonic reliability.

MEASUREMENT MODEL

The measurement model can be expressed in the condensed form

$$F = R * T * D * P * A \qquad (1)$$

where F is the measured signal from a defect, R is a reference waveform (e.g., back-surface echo), T accounts for interface transmission coefficients, D is a diffraction correction, P includes attenuation and phase change, and A is the scattering amplitude for the defect. This model has been verified for immersion testing via piston-source illumination of a variety of defects, such as spherical inclusions (1) and

cracks (2) in thermoplastic resin samples (9). More recently, diffusion bonded samples of IN100 and titanium alloy containing simulated circular and square cracks have been made available to us for additional testing (10). A number of results from these samples will appear later in this paper and elsewhere in these proceedings (11).

Further evolution of the measurement model will involve modelling of full-field radiation patterns using expansions in terms of orthogonal functions, such as Gaussian-Hermite functions. As a preliminary step, the first term in such a series, the simple Gaussian profile, has been implemented (8). This implementation involves a small-angle, or Fresnel approximation and incorporates passage of the ultrasonic beam through liquid-solid interfaces. The effects of aberrations of the beam profile caused by oblique incidences upon the interface are not included at present. As noted elsewhere in these proceedings (12), with proper normalization, this model closely approximates both the amplitude and beam width of a piston transducer in the far field. A fortunate implication is that modeling of the fields near the focal region of a focussed probe or focussing surface is therefore possible using Gaussian profiles. As an example, Figure 1 shows a comparison of the Gaussian model and experimental data using a 1/4-inch diameter unfocussed 10 MHz transducer and obtained from a transverse scan of a small bubble at the focus of a cylindrical (3 inch radius of curvature) surface in a fused quartz sample at normal incidence. Shown in the figure is the normalized amplitude of the spectral components at 5, 10 and 15 MHz. As can be seen, the Gaussian theory quite accurately predicts the transverse beam dimensions of the experimental data. Additional experimental comparisons will appear in a forthcoming report in the open literature.

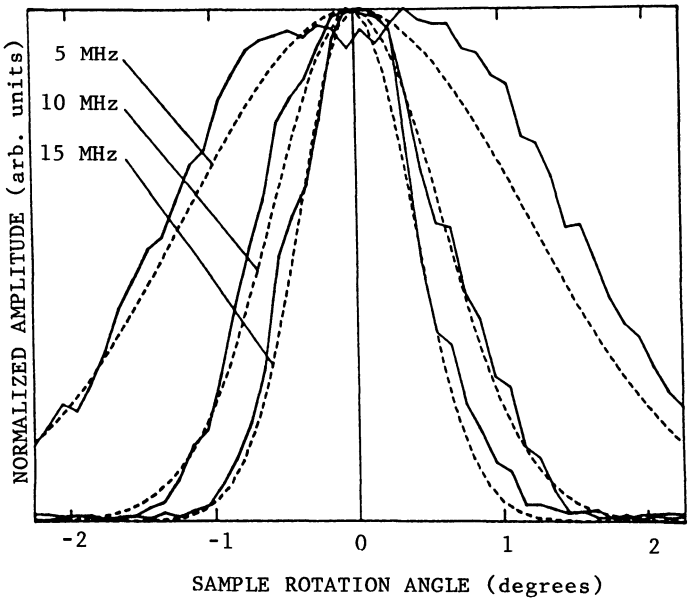

Fig. 1. Comparison of Gaussian theory (dashed line) and experiment (solid line) for scan of a spherical void below a concave 3 inch radius cylindrical interface.

APPLICATIONS

A number of important applications of measurement modeling to ultrasonic reliability have been mentioned in the introduction. In addition, two further applications which consider sizing of cracks (11) and modeling of scattering from branched intergranular stress corrosion cracks (13) are reported elsewhere in these proceedings. Two other new applications will be presented here.

First, an important use of modeling is to extrapolate meager experimental data, e.g., such as is used for system calibration, to cases not covered by experiment and identify any pitfalls created by the pecularities of calibration specimens. As an example, diffusion bonded titanium and IN100 samples containing simulated circular and square cracks were recently obtained by us. The circular cracks were machined parallel to the diffusion bond plane and sample surface while the square cracks are EDM notches perpendicular to the bond plane and have areas equal to the circular cracks. A possible use of these samples would be to predict the performance of an NDE system for detection of circular cracks. It might be hoped that signals from the circular simulated cracks would correlate to similarly oriented real cracks and that signals from the square EDM flaws would be close to those measured from real circular cracks perpendicular to a part surface.

Tests performed on the circular simulated cracks showed that this calibration approach was quite viable for determining detectability of circular cracks parallel to a part surface. For example, Fig. 2. shows the raw RF waveform and corresponding frequency spectrum for L-L backscatter from the circular defect (diameter=.030 in.) in the IN100 sample at a 30 degree incident angle relative to the crack normal. In addition, simulated results from the measurement model, on the same absolute scale, are shown which use exact theoretical results for the crack scattering amplitude using MOOT (14) and an approximate theory using the Kirchhoff approximation (15). As can be seen, the theoretical and experimental signal amplitudes agree quite well. Figure 3 shows a compilation of the results from the circular crack in the IN-100 sample, compared to the MOOT and Kirchhoff models, for a range of angles from normal (0-degree) to 60 degrees from normal to the crack. These plots were obtained by picking the rectified peak amplitude of the measured and simulated signals at each angle. Excellent agreement was observed over the range of angles utilized in the experiments.

However, test results from the square simulated cracks differed quite dramatically from those expected from model calculations. As can be seen in Fig. 4, the measured signal amplitudes were consistently larger than those predicted by theories for square or circular flat cracks. (Note in Fig. 4, the theoretical curves for circular cracks were generated assuming the same crack face area as the square crack, which was .027 inch on a side.) The cause of this discrepancy was believed to be due to scattering from the top of the EDM notch which had finite width (0.003"). Therefore, a model for scattering from a "box" was developed using the Kirchhoff approximation which included the top of the EDM notch. The resulting amplitude curve is also shown in Fig. 4. The agreement with measured values is still not precise, but the "box" theory does exhibit the same variation with illumination

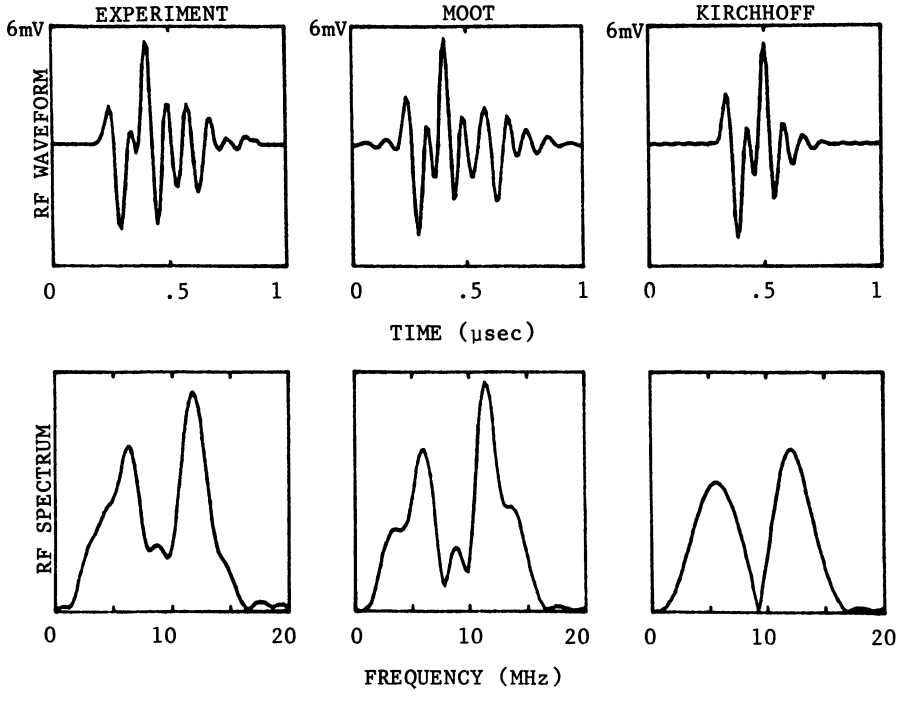

Fig. 2. Comparison of experimental and simulated RF waveforms and frequency spectra for longitudinal wave backscatter from a circular crack in IN100 at 30° incidence.

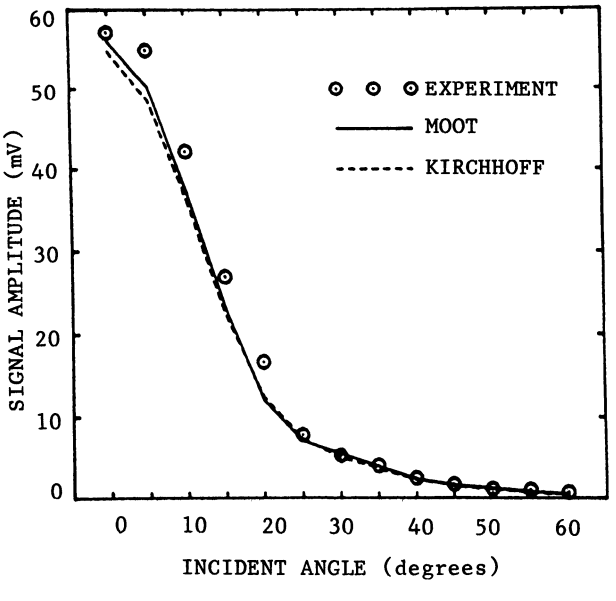

Fig. 3. Comparison of experimental (open circles) and simulated (solid line = MOOT, dashed line = Kirchhoff) peak signal amplitudes for a circular crack in IN100 as a function of illumination angle.

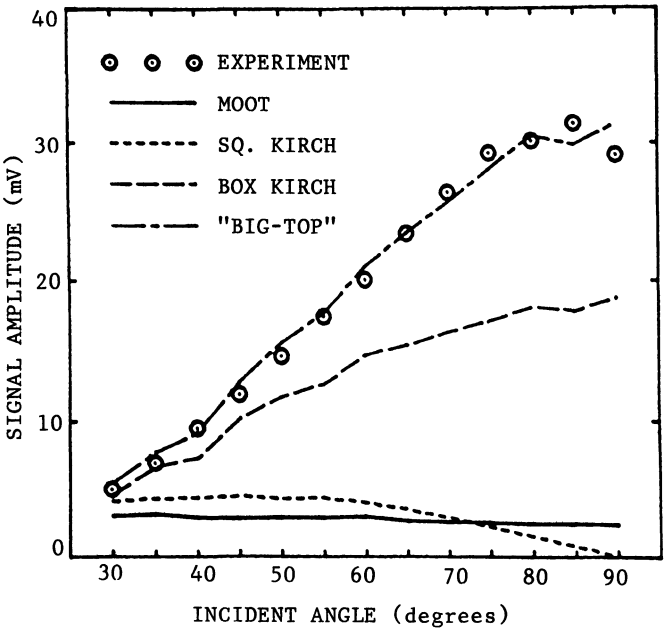

Fig. 4. Comparison of experimental and simulated signal amplitudes for a rectangular crack perpendicular to a planar surface in IN-100.

angle as does the experimental data. The difference between the experimental and "box" results could be due to imperfect bonding at the mouth of the EDM notch which produces a larger "top" to the simulated crack. Such a case was simulated assuming a top roughly 25% larger in area than the EDM mouth. As shown in Fig. 4, this gave essentially exact agreement to the experimental results.

Two important observations can be made about these results. First, the adequacy of the models in predicting the measured scattering from the circular "cracks" which were parallel to the sample surface lends credence to their use in predicting the scattering from circular cracks perpendicular to the surface since the same physical principles are involved. Second, these results also showed that the use of EDM notches to predict detection reliability for circular cracks is not appropriate. Furthermore, the model simulations show why this approach is inadequate due to the strong scattering from the "top" of the simulated square cracks.

The second application of modeling to ultrasonic reliability is a preliminary example of the use of Gaussian beam theory to predict the response of a scanned ultrasonic system. In this example, a 1/2-inch diameter, 5 MHz focussed probe (focal length = 4 inches in water) was used to scan a small bubble below the planar surface of a fused quartz sample. The immersion probe was inclined at a 7.2 degree angle relative to the sample surface to produce a 30 degree refracted angle and the focal plane was positioned at the depth of the bubble.

An x-y scan parallel to the sample surface was performed with 0.01" increments in both directions. The probe was inclined in the x-z plane (z is normal to the sample surface). At each scan position, the signal from the bubble was digitized and the spectral component at 5 MHz was recorded and the scan data was normalized to unity at maximum amplitude. Figure 5 shows the scan contours of 25%, 50% and 75% of peak amplitude for the experimental data and the corresponding Gaussian theory predictions with good agreement between results. Of course, a single frequency component is not appropriate to completely characterize such a scan. At this time, software to fully implement the Gaussian theory into the measurement model is being developed. This will allow absolute comparisons of simulated broad band signal amplitudes to measured scan data.

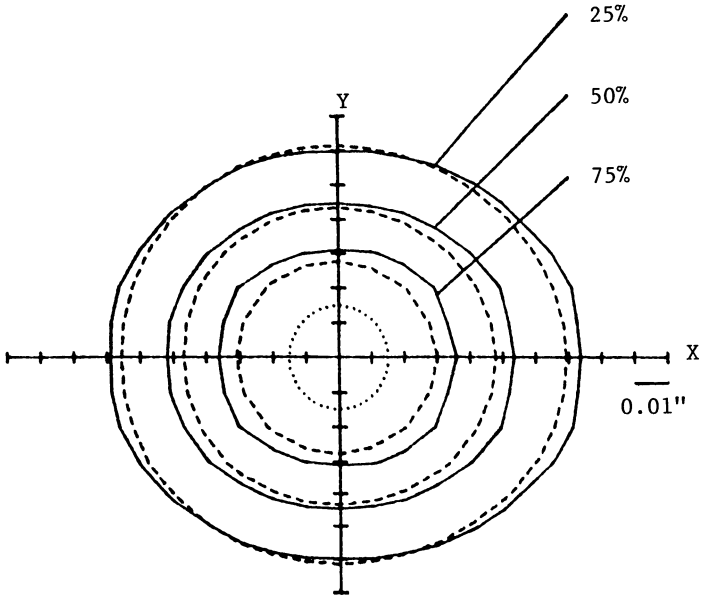

Fig. 5. Comparison of experimental (solid line) and Gaussian theory (dashed line) amplitude contours for an x-y scan of a bubble in glass. (Dotted line is outline of bubble).

SUMMARY

The use of Gaussian beam theory has been made in conjunction with the measurement model to predict full-field characteristics of ultrasonic inspections. When implementation is complete, the resulting model will allow simulation of scanned ultrasonic systems in which the flaws do not necessarily lie on the axis of the illuminating beam. Furthermore, the Gaussian profile is the first order term in Gaussian-Hermite and Gaussian-Laguerre expansions which may find applicability to extending measurement model analysis of piston source probes to the full-field, rather than just axial fields as is currently the case.

ACKNOWLEDGEMENT

This work was sponsored by the Center for Advanced Nondestructive Evaluation, operated by the Ames Laboratory, USDOE, for the Air Force Wright Aeronautical Laboratories/Materials Laboratory under Contract No. W-7405-ENG-82 with Iowa State University.

REFERENCES

1. R. B. Thompson and T. A. Gray, J. Acoust. Soc. Am. 74(4), 1983, p. 1279-1290.
2. R. B. Thompson and T. A. Gray, Review of Progress in Quantitative NDE 3, 1984, p. 373-383.
3. J. H. Rose, T. A. Gray, R. B. Thompson and J. L. Opsal, Review of Progress in NDE 2, 1983, p. 1065-1096.
4. T. A. Gray and R. B. Thompson, ibid, p. 89-112.
5. R. K. Elsley, R. C. Addison and L. J. Graham, ibid, p. 113-128.
6. K. W. Fertig, J. M. Richardson and R. K. Elsley, Review of Progress in Quantitative NDE 3, 1984, p. 65-80.
7. R. B. Thompson and T. A. Gray, Review of Progress in Quantitative NDE 2, 1983, p. 567-585.
8. R. B. Thompson and E. F. Lopes, J. Nondestr. Eval. (in press).
9. D. K. Hsu, C. Y. She, and Y. Li, Review of Progress in Quantitative NDE 3, 1984, p. 263-268.
10. Samples courtesy of R. L. Shambaugh, Pratt & Whitney Aircraft.
11. T. A. Gray and J. H. Rose, these proceedings.
12. R. B. Thompson and E. F. Lopes, these proceedings.
13. J. D. Achenbach, K-Y. Hu, A. N. Norris, T. A. Gray and R. B. Thompson, these proceedings.
14. J. Opsal, private communication.
15. L. Adler and J. D. Achenbach, J. Nondestruc. Eval., 1, 1980, p. 87-99.